

TITAN ZONAL WIND CORROBORATION VIA THE HUYGENS DISR SOLAR ZENITH ANGLE MEASUREMENT

Michael Allison⁽¹⁾, David H. Atkinson⁽²⁾, Michael K. Bird⁽³⁾, Martin G. Tomasko⁽⁴⁾

⁽¹⁾NASA/Goddard Institute for Space Studies; 2880 Broadway; New York, NY 10025 (U.S.A.),

Email: mallison@giss.nasa.gov

⁽²⁾Department of Electrical and Computer Engineering; University of Idaho; Moscow, ID 83844 (U.S.A.),

Email: atkinson@ece.uidaho.edu

⁽³⁾Radioastronomisches Institut; Universität Bonn; Auf dem Hügel 53121 Bonn (Germany),

Email: mbird@astro.uni-bonn.de

⁽⁴⁾Lunar and Planetary Laboratory; University of Arizona; Tucson, AZ 85721 (U.S.A.),

Email: mtomasko@lpl.arizona.edu

ABSTRACT

The *in situ* measurement of the vertical profile of Titan's zonal wind is a major objective of the Huygens probe mission, as specifically addressed by the Doppler Wind Experiment (DWE). It now appears likely that an independent, if somewhat less accurate corroboration of the zonal wind retrieval will be afforded by the measured variation of the solar zenith angle Z from the Huygens Descent Imager/Spectral Radiometer (DISR) throughout the course of the probe's atmospheric descent. The analyzed synergism of the DWE and DISR solar- Z measurements should provide an enhanced evaluation of the Titan atmospheric circulation.

1. INTRODUCTION

The inference of a global cyclostrophic circulation on Titan, based on the colder-poleward gradient of stratospheric temperatures revealed by Voyager infrared measurements [1], makes Saturn's atmospheric satellite an especially important target for *in situ* wind measurements. Although Titan's atmospheric super-rotation has been further evidenced by stellar occultation measurements of the oblate deformation of its upper level isobars [2] and the spectroscopic Doppler-shift of a 12 μ m ethane line [3], the observations are not spatially well-resolved and admit to uncertainties in the zonal wind as large as several tens of meters per second. While important progress has been made in the development of numerical general circulation models (GCMs) for Titan [4-8], providing an explicit realization of the upward transport of angular momentum by a global meridional cell similar to that originally proposed by Gierasch for Venus [9], these show large differences in the size, strength and vertical arrangement of the circulation. Progress in understanding the roles of thermal tides [10], seasonal-dynamical inertia [11], the Saturn gravitational tide [12], boundary layer [13], and

potential vorticity mixing [14] in the maintenance of Titan's circulation will depend on accurate and spatially resolved measurements of the wind itself.

The Huygens Doppler Wind Experiment (DWE) is specifically dedicated to providing a highly resolved measurement of the vertical profile of the zonal wind at the probe's south-equatorial entry site to within an accuracy better than ~ 1 m/s [15]. This will provide a "ground-truth" benchmark for thermal wind mapping of Titan's global circulation from the Cassini Composite Infrared Spectrometer [16] as well as cloud-tracked wind measurements from the Cassini Imaging Science Subsystem [17] and Visual Infrared Mapping Spectrometer [18]. The DWE measurement will also be key to the retrieval of the Huygens descent trajectory and the determination of the probe landing site.

While the DWE is expected to provide the single-most accurate measurement of the Huygens wind-drift, the technique is strictly dependent upon the relative geometry of the Cassini orbiter and probe, and therefore admits a convolution of the registered zonal motion with the descent velocity, as well as any meridional winds. Given the importance of the wind drift to both the meteorology and probe tracking, it seems desirable to consider independent measurements from Huygens. Accelerometry data from the Huygens Atmospheric Structure Instrument (HASI) will register wind gusts [19], and their time integration may provide a crude measure of accumulated zonal drift. The Descent Imager Spectral Radiometer (DISR) may provide an ancillary measure of wind drift by the time-lapse tracking of discrete surface features visible in its panoramic mosaics [20]. This paper explores the possibility that DISR measurements of the solar zenith angle Z will provide a further check on the zonal wind profile, less affected than the DWE by the probe descent velocity, and with a different dependence on meridional motion.

2. HUYGENS SOLAR ZENITH ANGLES

Both Titan's rotation and an eastward (prograde) wind-drift will impose an apparent decrease in the solar zenith angle Z with time, as observed by the Huygens probe. According to the ground test results [20], DISR can measure the solar Z to within $0^\circ.2$, as averaged over the short period oscillations associated with the swing and rotation of the probe under its parachute. The measured rate of decrease of the solar Z by Huygens to the anticipated precision will therefore provide a check on the Doppler measured wind-drift, independent of the

probe-orbiter geometry. Fig. 1 shows the latitude-longitude dependence of the solar Z on Titan at the time and vicinity of the Huygens atmospheric entry, as calculated with the algorithm outlined in the Appendix. As with the DWE, the wind-drift evaluated from the measured solar Z will admit to some ambiguity between zonal and meridional motion. It is of interest to note, however, that the previously considered 11°N latitude entry for the Huygens probe entry would have been less favorable to the solar- Z reckoning, since as Fig. 1 shows, this measured angle is a steeper function of the latitude there, and less rapidly varying with longitude.

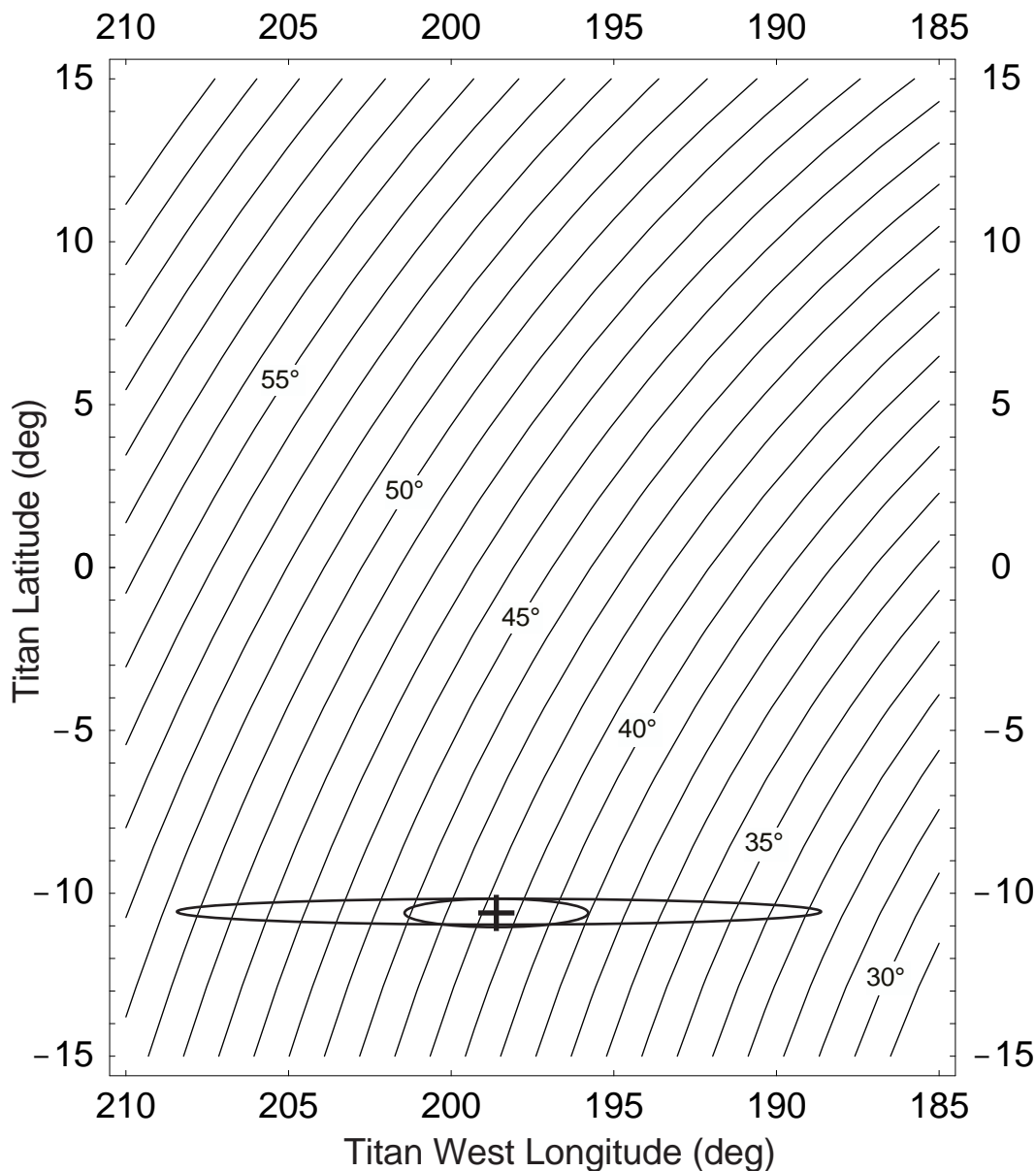


Fig. 1. The variation of the solar zenith angle Z with latitude and longitude at the time t_0 of the Huygens parachute descent. The target coordinates ($10^\circ.7\text{ S}$, $198^\circ.6\text{ W}$) are marked with a cross. The small ellipse shows the anticipated $1-\sigma$ delivery error, while the larger ellipse characterizes the range of landing sites implied by the engineering wind envelope.

As pointed out by Atkinson and Kazeminejad [21], the error ellipse for the Huygens probe delivery, as indicated in Fig. 1, can itself be “circularized” to within $\sim 0.6^\circ$ in longitude by the DISR solar-Z measurement. The proposed solar-Z wind tracking is simply an extension of this optical navigation method to the time-rate-of-change of the probe motion over longitude.

3. HUYGENS DESCENT AND WIND MODELS

Anticipated time-altitude profiles for the Huygens probe descent are shown in Fig. 10 of the mission review by Lebreton and Matson [22]. The current uncertainty in the actual vertical profile of Titan’s atmospheric density implies a possible variation of $\sim \pm 16$ min with respect to a nominal descent time of 137 min. The altitude of the nominal descent (in km) as a function of the descent time (in hr) can be represented to good approximation with the polynomial expression

$$z_{\text{probe}} \approx [198.7 - 378.8 \cdot \text{hr} + 331.4 \cdot \text{hr}^2 - 138.0 \cdot \text{hr}^3 + 21.4 \cdot \text{hr}^4] \text{ km} \quad (1)$$

This provides a simple estimate of the anticipated altitude of the Huygens probe well within the upper and lower bounds of the long and short descent envelopes shown by Lebreton and Matson.

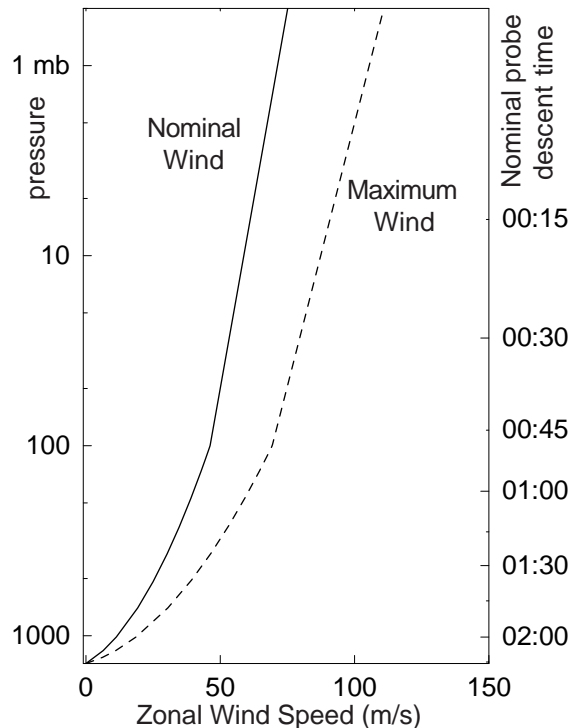


Fig. 2. Titan engineering wind models [23], as evaluated for the Huygens probe entry latitude.

Engineering envelopes for the Titan zonal wind were devised by Flasar, Allison, and Lunine [23] in support of the design of the Huygens descent trajectory. Fig. 2 shows the vertical profiles of both the “nominal” and “ $2 \times \Delta T$ ” envelope (which assumes a latitudinal temperature contrast twice that observed by the Voyager infrared experiment) as evaluated for the $10^\circ.7$ South latitude of the Huygens entry.

Since the engineering wind model is given in terms of the pressure level, but our model for the descent altitude of the probe is given, as in Eq. 1, in terms of the geometrical elevation, we must specify a conversion between elevation and pressure (or log-pressure) for the integrated calculation of the model probe wind drift. This is of course given by the integration of the vertical hydrostatic law, assuming an ideal gas atmosphere, and should include an account of the variation of both the temperature and gravitational acceleration with height. For computational facility, we have fitted a simple cubic polynomial function to this hydrostatic calculation of the log-pressure scale height, of the form

$$\ln(p/p_s) \approx 0.0694 z - 2.65 \times 10^{-4} z^2 + 4.69 \times 10^{-7} z^3 \quad (2)$$

where z is the elevation in km and $p_s \approx 1.4$ bar is the surface pressure of Titan. The substitution of Eq. 1 into Eq. 2 then provides an estimate of the log-pressure level of the Huygens probe as a function of time, as indicated along the right-side ordinate of Fig. 2. With the analytic wind profile equations specified by the engineering model [23] these also provide representative estimates of the time-dependent probe drift velocity.

Although GCM experiments [7], theoretical arguments [24], and the measured spectroscopic shift of Titan’s ethane line [3] all indicate a prograde, eastward zonal flow on Titan, the cyclostrophic thermal wind balance is strictly indeterminate as to the direction of the circulation and the Huygens Project has therefore planned for the possibility of both westward and eastward probe drift. We will also consider both these cases here.

4. SOLAR-Z WIND TRACKING

Assuming a latitude fixed at the Huygens entry target, the linearization of the solar Z dependence on time and longitude implies

$$Z_{\text{Huygens}} \approx -132^\circ.06 - 0.856(^\circ/\text{hr}) \cdot h_U + 0.9138 \cdot \phi_T \quad (3)$$

where h_U represents the decimal UTC hour (SCET) on 2005 Jan 14 and ϕ_T is the west Titan longitude [cf. Eq. A12 in the appendix.] Fig. 3 shows a contour plot

of the resulting solar-Z dependence upon longitude and time at the Huygens target latitude. Upon differentiation of Eq. 3 with respect to time and rearrangement, the time-rate-of-change of the probe longitude can be related to the time-rate-of-change of the measured solar-Z as

$$d\phi_T/dh_U \approx 1.094 \cdot dZ_{\text{Huygens}}/dh_U + 0.936^\circ/\text{hr}. \quad (4)$$

But the drift velocity $U \equiv -\frac{\pi a \cos \theta_{\text{Huygens}}}{180^\circ} \left(\frac{1 \text{ hr}}{3600 \text{ s}} \right) \frac{d\phi_T}{dt}$

(signed minus for Titan West Longitude ϕ_T) where $a = 2575 \times 10^3 \text{ m}$ is the Titan equatorial radius. Then in terms of a measured time-rate-of-change \dot{Z} for the solar zenith angle, given in deg/hr, the implied zonal wind velocity for the Huygens probe is simply

$$U \approx - (13.5 \text{ hr/deg } \dot{Z} + 11.5) \text{ m/s}. \quad (5)$$

Note that the second term on the right is just Titan's equatorial rotation speed! Of course the interpretation of this drift velocity as a pressure-level profile requires a specified pressure-level dependence for \dot{Z} . But this information should be provided directly by HASI.

As an illustration of the likely measured range of the solar-Z variation by Huygens, Fig. 3 also shows as the heavy dashed curves its time-longitude dependence for the nominal and maximum engineering wind models,

for both a prograde (eastward drifting) and a retrograde circulation. The vertical dashed line corresponds to the unlikely case of no wind.

5. PROSPECTS

It should be recognized that the solar-Z wind tracking technique really measures the *time integrated* velocity (i.e. the drift distance with descent time) which can then be interpreted as a *time-averaged* velocity. By reference to Eq. 5, an error of $\delta Z \sim 0.2^\circ$ over 1 hour, for example, would correspond to an error in the averaged velocity of $\sim 3 \text{ m/s}$, while over 30min, the same δZ would imply an error of $\sim 6 \text{ m/s}$. In these terms, the technique may therefore be regarded as a fairly "good" measure of wind velocity but at a relatively poor vertical resolution. Other sources of error may degrade the wind-drift analysis. Atmospheric refractivity, for example, may also affect the solar-Z (R. Lorenz, personal communication), but probably with only a very small differential variation. A further unstudied possibility, however, is that DISR scans of the horizon may determine the tip of the probe perpendicular to the plane containing both the zenith and the Sun and therefore provide an estimate of the latitudinal drift. In any event, the complementary constraints afforded by the DISR-DWE synergism should provide a higher level of confidence for the Huygens zonal wind retrieval.

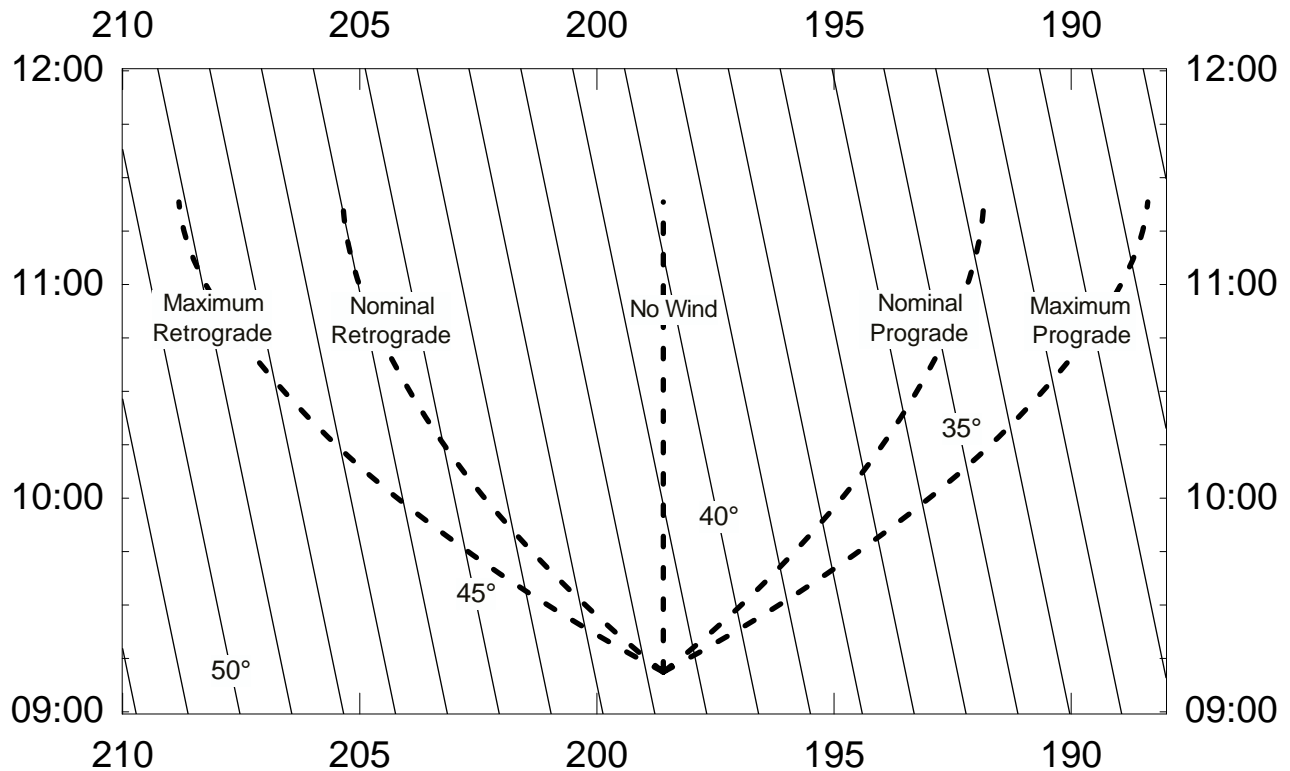


Fig. 3. Titan solar zenith angles as a function of west longitude and the time in UTC (SCET) on 2005 Jan 14. The heavy dashed lines show the longitude-time variation of the Huygens solar-Z for the engineering wind models.

APPENDIX: TITAN SUB-SOLAR COORDINATE AND ZENITH ANGLE ALGORITHM

As referenced to a Barycentric Dynamical Time (TDB) argument T measuring Julian centuries elapsed post-J2000 (JD2451545.0), the following algorithm provides an efficient calculation of Titan's planetocentric solar longitude L_S , sub-solar longitude-latitude coordinates (Λ_S, δ_S), and μ the cosine of the local solar zenith angle Z , for a Titan planetographic west longitude ϕ_T and latitude θ_T . Starting with the evaluation of T in terms of the UTC Julian Date (JD_{UTC}),

$$T = (JD_{UTC} - 2451545.0)/36525 + 1.2 \times 10^{-8} [(JD_{UTC} - 2451545.0)/36525 + 1.3]^2, \quad (A1)$$

where the second term provides an approximate conversion from the UTC to TDB time scales. Then,

$$M = 316^\circ.91 + 1222^\circ.08T \quad (A2)$$

$$\alpha_{FMS} = 236^\circ.64 + 1223^\circ.22T \quad (A3)$$

$$\epsilon = 26^\circ.40 - 0^\circ.07T \quad (A4)$$

$$V_m = 321^\circ.18 + 824624^\circ.55T \quad (A5)$$

$$L_S = \alpha_{FMS} + (6^\circ.36 - 0^\circ.04T) \sin M + 0.22 \sin 2M + 0.01 \sin 3M + 0.19 \cos(1182^\circ.44T + 24^\circ.1) + 0.12 \cos(591^\circ.22T + 13^\circ.9) + 0^\circ.04 \sin(V_m - \alpha_{FMS}) \quad (A6)$$

$$\alpha_S = L_S + \frac{180^\circ}{\pi} \sum_{n=1}^3 \frac{1}{n} \left(-\left(\tan \frac{\epsilon}{2} \right)^2 \right)^n \sin(2nL_S) \quad (A7)$$

$$\Lambda_S = \text{Mod}[V_m - \alpha_S, 360^\circ] \quad (A8)$$

$$\delta_S = \text{ArcSin}(\sin \epsilon \sin \Lambda_S) \quad (A9)$$

$$H_S = \Lambda_S - \phi_T \quad (A10)$$

$$\mu \equiv \cos Z = \sin \theta_T \sin \delta_S + \cos \theta_T \cos \delta_S \cos H_S \quad (A11)$$

M represents the solar mean anomaly, α_{FMS} the right ascension of the "Fictitious Mean Sun" [25] and ϵ the obliquity of Titan's equator with respect to its mean solar orbit. V_m represents the prime meridian "hour angle" measured with respect to Titan's own vernal equinox, as converted from the angle W measured with respect to the "Q" node. L_S is Titan's planetocentric solar longitude (0° at the vernal equinox), evaluated here as a series expansion for the "equation of center," and α_S is the true solar right ascension.

The algorithm incorporates the largest few planetary perturbations on Saturn's longitude [26] as well as Titan's moving orbital position. Its simplified time-linear representation of the planetocentric mean elements is intended only for applications within the one-century interval 1950 – 2050 ($|T| \leq 0.5$). Extensive checks of the algorithm against the SPICE calculator posted at <http://alphie.tucson.az.us/spiceweb/> indicate that its output values for the sub-solar coordinates on Titan are in error by no more than $0^\circ.03$ for the years 1967 – 2012. As evaluated for the Huygens mission epoch, the agreement is fortuitously within $0^\circ.01$, a smaller difference than the uncertainty in Titan's pole vector!

The nominal t_0 for the Huygens entry is 2005 Jan 14 9:11:10.8 UTC, Spacecraft Event Time (SCET), or JD_{UTC}2453384.882764. Although both the UTC clock time and Julian Date can be converted to the corresponding dynamical or ephemeris time (TDB), Eq. A1 provides its own approximate conversion to this, as measured by the centennial argument T . These times should not be confused with the "Earth Receive Time" (ERT), on this date some 67min later.

As evaluated for the Huygens t_0 , the planetocentric solar longitude is $L_S = 300^\circ.53$ (mid-northern winter). It may be noted that Titan's obliquity and L_S are both slightly different than Saturn's, by a small, temporally varying amount (\sim a few tenths of a degree), as a result of the slow (691yr) oscillation of its Saturn orbit about the Laplacian plane, as built into the assumed specification of Titan's pole vector [27]. Again at Huygens t_0 the sub-solar point on Titan is at $\Lambda_S = 156^\circ.85$ W and $\delta_S = 22^\circ.52$ S. For the targeted Huygens entry at $198^\circ.6$ W longitude and $10^\circ.7$ S latitude, the local solar zenith angle at the start of the mission is $Z(t_0) = 41^\circ.56$.

Although Eqs. A1 – A11 are easily encoded for numerical evaluation, parametric studies of the slowly changing solar Z over the course of the Huygens mission may also be referred to a still simpler prescription. For any time within several hours of the Huygens t_0 , and for any Titan planetographic coordinate position within some 10° of the target longitude and 2° of the target latitude, the solar Z can be estimated (to within $\sim 0^\circ.1$) by a linearization of (A1) – (A11) as

$$Z_{\text{Huygens}} \approx 43^\circ.26 - 0^\circ.856 (h_U - 9) + 0^\circ.911 (\phi_T - 200^\circ) + [0^\circ.380 - 0^\circ.004 (\phi_T - 200^\circ)] (\theta_T + 10^\circ). \quad (A12)$$

Here the h_U variable represents the decimal UTC hour (SCET) on 2005 Jan14 (e.g. $h_U = 9.1863$ at the nominal Huygens t_0), and again ϕ_T is the Titan west longitude and θ_T the Titan latitude.

ACKNOWLEDGMENTS

The authors acknowledge the support of the European Space Agency and the National Aeronautics and Space Administration through the Cassini/Huygens Project.

REFERENCES

1. Flasar, F.M., Samuelson, R.E., and Conrath, B.J. Titan's atmosphere: temperature and dynamics. *Nature* Vol. 292, 693-698, 1981.
2. Hubbard, W.B. *et al.* The occultation of 28 Sgr by Titan. *Astron. Astrophys.*, Vol. 269, 541-563, 1993.
3. Kostiuk *et al.*, Direct measurement of zonal winds on Titan. *Geophys. Res. Lett.* Vol. 28, 2361-2364, 2001.
4. Hourdin, F. *et al.* Numerical simulation of the circulation of the atmosphere of Titan. In *Symposium on Titan. ESA SP-338*, 1992.
5. Del Genio, A.D., Zhou, W., and Eichler, T.P. Equatorial superrotation in a slowly rotating GCM: Implications for Titan and Venus. *Icarus*, Vol. 101, 1-17, 1993.
6. Hourdin, F. *et al.* Numerical simulation of the general circulation of the atmosphere of Titan. *Icarus*, Vol. 117, 358-374, 1995.
7. Del Genio, A.D. and Zhou, W. Simulations of superrotation on slowly rotating planets: sensitivity to rotation and initial condition. *Icarus*, Vol. 120, 332-343, 1996.
8. Tokano, T. *et al.* Seasonal variation of Titan's atmospheric structure simulated by a general circulation model. *Planet. Space Sci.* Vol. 47, 493-520, 1999.
9. Gierasch, P.J. Meridional circulation and the maintenance of the Venus atmospheric rotation. *J. Atmos. Sci.* Vol. 32, 1038-1044, 1975.
10. Leovy, C. Zonal wind in the stratosphere of Titan. In *The Atmospheres of Saturn and Titan. ESA SP-241*, 95-98, 1985.
11. Flasar, F.M. and Conrath, B.J. Titan's stratospheric temperatures: a case for dynamical inertia. *Icarus*, Vol. 85, 346-354, 1990.
12. Tokano, T. and Neubauer F.M. Tidal winds on Titan caused by Saturn. *Icarus* Vol.158, 499-515, 2002.
13. Allison, M. A preliminary assessment of the Titan planetary boundary layer. In *Symposium on Titan. ESA SP-338*, 113-118, 1992.
14. Allison, M., Del Genio, A.D. and Zhou, W. Zero potential vorticity envelopes for the zonal-mean velocity of the Venus/Titan atmospheres. *J. Atmos. Sci.* Vol.51, 694-702, 1994.
15. Bird, M.K., *et al.* The Huygens Doppler Wind Experiment *Space Sci. Rev.* Vol.104, 613-640, 2002.
16. Flasar, F.M. *et al.* Exploring the Saturn system in the thermal infrared: The composite infrared spectrometer. *Space Sci. Rev.* (in press), 2004.
17. Porco, C. *et al.* The Cassini Imaging Science Investigation. *Space Sci. Rev.* (in press), 2004.
18. Brown, R. *et al.* The Cassini Visual Infrared Mapping Spectrometer. *Space Sci. Rev.* (in press), 2004.
19. Fulchignoni, M. *et al.* The characterization of Titan's atmospheric physical properties by the Huygens Atmospheric Structure Instrument (HASI). *Space Sci. Rev.* Vol.104, 395-431, 2002.
20. Tomasko, M.G., *et al.* The Descent Imager/Spectral Radiometer (DISR) Experiment on the Huygens Entry Probe of Titan. *Space Sci. Rev.* Vol.104, 469-551, 2002.
21. Atkinson, D.H. and Kazeminejad, B. Huygens Descent Trajectory Working Group Report, 2003. <<http://huygens.oaew.ac.at/DTWGpapers.html>>.
22. Lebreton, J.-P. and Matson, D.L. The Huygens probe: science, payload, and mission overview. *Space Sci. Rev.* Vol.104, 59-100, 2002.
23. Flasar, F.M., Allison, M.D., Lunine, J.I. Titan zonal wind model. In *Huygens: Science, Payload and Mission. ESA SP-1177*, 298-298, 1997.
24. Flasar, F.M. The dynamic meteorology of Titan. *Planet. Space Sci.* Vol.46, 1125-1147, 1998.
25. Allison, M. and Ferrier, J., Planetocentric solar coordinates including simplified recipes for seasonal/diurnal timing on Saturn and Titan. (In preparation.)
26. Simon, J.L. *et al.* Numerical expressions for precession formulae and mean elements for the Moon and the planets. *Astron. Astrophys.* Vol.282, 663-683, 1994.
27. Seidelmann, P.K. *et al.* Report of the IAU/IAG working group on cartographic coordinates and rotational elements of the planets and satellites: 2000. *Celest. Mech. Dynam. Astron.* Vol.82, 83-110, 2002.

Corrigendum

The print-published version of this paper contained a typographical error in Eq.(A7). As printed, the minus sign appearing in

$$\alpha_s = L_s + \frac{180^\circ}{\pi} \sum_{n=1}^3 \frac{1}{n} \left((-\tan \frac{\epsilon}{2})^2 \right)^n \sin(2nL_s) \quad (A7)$$

should have appeared outside of the small parenthesis. The correct equation:

$$\alpha_s = L_s + \frac{180^\circ}{\pi} \sum_{n=1}^3 \frac{1}{n} \left(-(\tan \frac{\epsilon}{2})^2 \right)^n \sin(2nL_s) \quad (A7)$$

appears in this reprint version of the paper, as given on the previous page.